Correlated diffraction and fluorescence in the backscattering iridescence of the male butterfly *Troides magellanus* (Papilionidae)

Jean Pol Vigneron,[1,*] Krisztián Kertész,[2] Zofia Vértesy,[2] Marie Rassart,[1] Virginie Lousse,[1] Zsolt Bálint,[3] and László P. Biró[2]
[1]*Laboratoire de Physique du Solide, Facultés Universitaires Notre-Dame de la Paix, rue de Bruxelles, 61, B-5000 Namur, Belgium*
[2]*Research Institute for Technical Physics and Materials Science, POB 49, H-1525 Budapest, Hungary*
[3]*Hungarian Natural History Museum, Baross utca 13, H-1088, Budapest, Hungary*
(Received 30 July 2007; revised manuscript received 23 May 2008; published 8 August 2008)

The male *Troides magellanus*—a birdwing butterfly that lives in a restricted area of the Philippines—concentrates on its hindwings at least two distinct optical processes that contribute to its exceptional visual attraction. The first is the very bright uniform yellow coloration caused by a pigment which generates yellow-green fluorescence, and the other is a blue-green iridescence which results from light diffraction at grazing emergence under a specific illumination. Detailed optical measurements reveal that these optical effects are correlated, the fluorescence being enhanced by illuminations conditions that favor the occurrence of the iridescence. These effects are analyzed, with the conclusion that both of them depend on the same optical device: a one-dimensional microribs grating which appear on the sides of the ridges that run along the yellow scales.

DOI: 10.1103/PhysRevE.78.021903 PACS number(s): 42.66.−p, 42.70.Qs, 42.81.Qb

I. INTRODUCTION

The "birdwings" comprise some of the largest butterflies on Earth [1]: the wingspan of some of them, such as *Ornitopthera alexandrae*, can reach 30 cm. The common name of these butterflies, "birdwings," has most probably been coined after the visual appearance of their wings, where a particular pattern of colors and the disposition of veins suggests the fake presence of feathers.

The "birdwings" essentially collect the genera Ornitopthera, Trogonoptera, and Troides [2–4], all placed by animal systematics in the tribe Troidini of the family of true butterflies (Papilionidae). With respect to larval host, Troidini offer the best examples of "oligophagy" in butterflies, which means that they are strictly dependent on a small variety of feeding plants—in the present case, the poisonous Aristolochiaceae [5]. The pressure on the area occupied by their rainforests severely limits the population of these insects and all birdwings" are classified as vulnerable or endangered [6]. The specimens used for our studies were all certified to have been obtained through commercial breeding or taken from the historical samples of the Hungarian Natural History Museum.

These large butterflies can be found in the subtropical and tropical zones of the Oriental and Australian zoogeographical regions. Their coloration is showy, with very contrasting shades of green, yellow, orange, black, and white. Blue and orange, and almost completely black species are also known. Except in a few species, such as *Ornithoptera paradisea*, the hindwings lack tails on their hindwings. The sexual dimorphism is strong, with females appreciably larger and less colorful than males. Adult birdwings are encountered in the rainforests, where they seek nectar-bearing flowers in the canopy [7]. They can also be encountered in the forest periphery, where they would feed on terrestrial flowers or mate [8]. They seem to be attracted by sunlit spots where to bask. In this situation, the very absorbing black areas catch much of the solar illumination and frequent wing reorientation moves, observed at that moment, are likely associated with some kind of thermal control.

The genus Troides has the widest distribution in Troidini, with a diversity of 17–22 species [2,4]. Two species in this genus, *Troides prattorum* (Joicey and Talbot, 1922) (restricted to the Indonesian Island Buru) and *Troides magellanus* (C. Felder and R. Felder, 1862) (distributed in the Philippines and Taiwan) display a curious optical phenomenon: the male adult butterflies—besides very absorbing, black, forewings—possess brightly colored yellow hindwings which, when looked upon from a very precise, grazing, angle, send a conspicuous white signal (sometimes showing bluish or greenish hues). As the present study shows, this phenomenon, occurring in the male *Troides magellanus* (see Fig. 1), is much more complex than indicated by the results of previous studies [9].

Indeed, another visual effect provided by this butterfly also occurs in the large yellow areas, the coloration of which is known to originate from a pigment called "papiliochrome." The yellow reflectance actually involves fluorescence, i.e., a mechanism by which ultraviolet radiation is absorbed and reemitted as greenish yellow. Fluorescence is rather common in the mineral world, but in the animal kingdom [10], it does not seem to be so frequent. As the present study shows, the fluorescence and the iridescence of the hindwings of *Troides magellanus* are actually correlated, and most of our investigations will focus on this correlation effect.

The flight of a male *Troides magellanus* is very peculiar, using essentially the forewings with ample propulsion movements, while the hindwings nearly keep still. This can serve a signaling strategy that uses the highly directional white emission.

The physics of the iridescence of the male *Troides magellanus* has been considered by Lawrence *et al.* [9]. The explanation rested on the concept of a "bigrating," a particular way of understanding the diffraction by a finite-thickness

*jean-pol.vigneron@fundp.ac.be

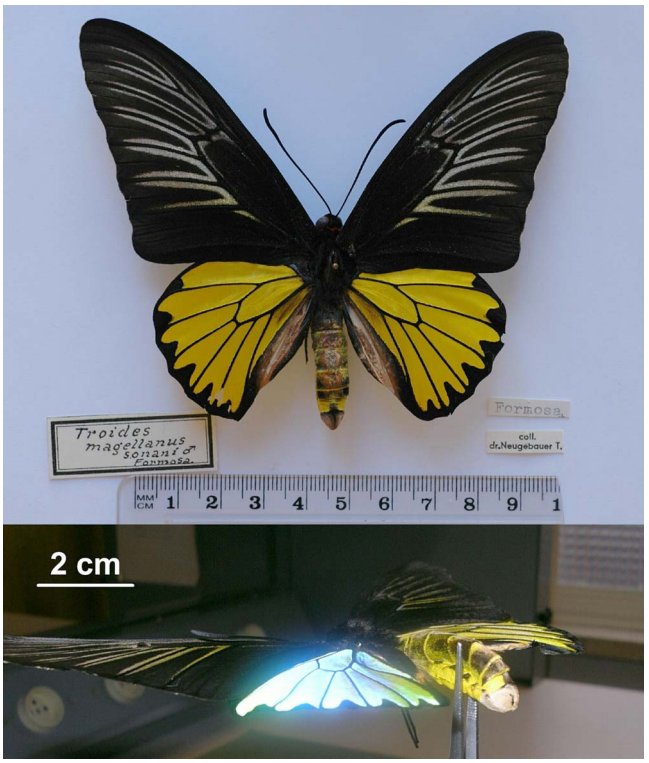

FIG. 1. (Color online) The male butterfly *Troides magellanus* is a large insect bearing black forewings and mostly yellow hindwings. The upper view shows the dorsal side of the butterfly, seen under near-normal incidence. The lower image shows the backscattered flash of white light seen when moving the butterfly plane close to the observation axis, in a grazing backscattering geometry.

oblique structure. We will not follow this analysis here, but rather interpret the observations in terms of a one-dimensional blazed grating which, in our opinion, better exploits the actual structure revealed by the scanning electron microscope. The optical measurements carried out in the present work, though compatible with those reported in Lawrence *et al.*, avoid the hemispheric integration and then provide more details on the scattering directions ruled by the scales structure. This deeper analysis of the optical properties calls for an extended interpretation and an improved physical model. Section II develops available and newly acquired knowledge on the structure of the yellow scales of the butterfly. Section III reports more specifically the optical measurements and their associated theoretical interpretations.

II. SCANNING ELECTRON MICROSCOPY

The ultrastructure of the yellow scales of the male *Troides magellanus* was revealed by the pioneering work of Lawrence *et al.* [9]. Though much of the ultrastructure is known, it appeared necessary to carry out new measurements of the geometry in order to extract the specific data required by our revised modeling. Most previously known results have been confirmed by these observations and other parameters, not yet reported, could be extracted.

A. Methods

For this morphology investigation, small pieces of butterfly wings were cut from the flat yellow regions between the veins of the hindwings of a male *Troides magellanus* and attached to the sample holder by double-sided carbon tape. In order to improve surface contrast and to prevent charging, sample were covered by a sputtered gold layer approximately 25 nm thick. Samples were investigated using two scanning electron microscopes (SEM): Philips XL 20 or LEO 1540 XB. Where needed, cross section slices (70 nm thick) were used to help visualizing the three-dimensional structure. These slices were prepared by embedding small yellow parts of the wings in EMbed 812 resin which were cut by an ultramicrotome. The slices were deposited on a grid for examination with a transmission electron microscope (FEI TECNAI).

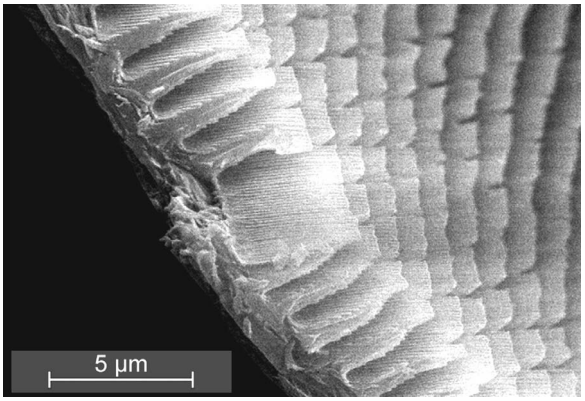

FIG. 2. General view of the surface of a dorsal yellow scale from the hindwing of the male *Troides magellanus*. The scale consists of an unstructured basal slab supporting an array of high-aspect-ratio parallel ridges. The ridges bear regularly spaced and slanted transversal microribs.

B. Results

A general view of the ultrastructure is shown on Figs. 2 and 3, which confirms the contents of the images described earlier [9]. High parallel ridges, with a triangular cross section, run along the length of the scales. Contrasting many

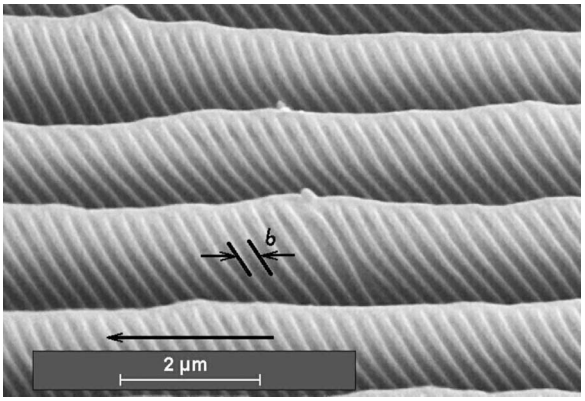

FIG. 3. Lateral view of the ridges from a dorsal yellow scale of the male *Troides magellanus*. The average slant angle of the microribs is 61° with respect to the ridge crest. The arrow points toward the scale pedicel, that is towards the body of the insect. The periodicity step is $b=261$ nm.

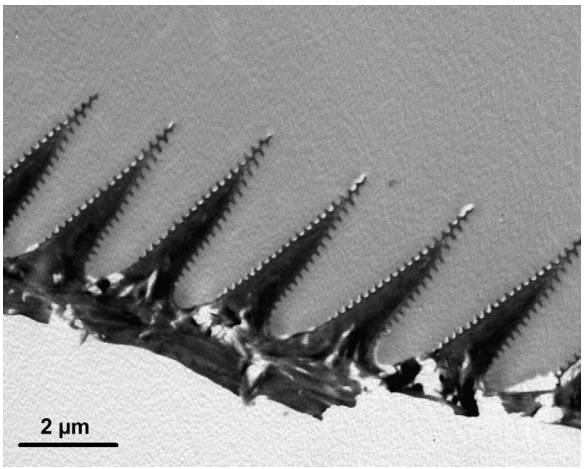

FIG. 4. Transmission electron microscope image of a cross section of the ridges array. Each ridge appears as a bulk strut with a triangular cross section. The side protrusions are sections of the microribs which appear to be a one-dimensional grating. Only the upper part of the scale is shown in the image.

other butterfly scales [9,11–17], the cross ribs are invisible. The ridges have evolved into a triangular rigid core, close to 3.8 μm high and 1.1 μm wide, near the base. The distance between the top edges of two neighboring parallel ridges is, on the average, close to 1.4 μm. The sides of these triangular ridges bear parallel protruding stripes called "microribs." These microribs are slanted at about 61° relative to the basal slab defining the scale plane or relative to the top edge of the ridges. Neglecting the small irregularities and the finite length of ridges, the one-dimensional periodic repetition of these microribs along the ridges implies a one-dimensional translational invariance of the ultrastructure of the scale, with a lattice parameter (along the top edge of the ribs) b =261 nm.

The information on the geometry of the ridge, drawn from SEM, can be confirmed by the examination of thin slices of the scales in transmission electron microscopy (TEM, see Fig. 4). The lower part of the scale is hollow, with a basal membrane on which the array of triangular ridges is erected. In TEM cross sections, the ridges appear as black triangles and the microribs are seen as narrow protrusions on the long triangles side. The thickness of the microribs can be estimated to be 88 nm. Each one is sticking out from each side of the ridge over an average distance of 114 nm, but they become rapidly less apparent near the basal plane.

III. LIGHT REFLECTION FROM THE YELLOW SCALES

The visual effects under investigation are rather complex, as we will see, and we will try to describe the observations in sequence, while providing the theoretical arguments that support our understanding of the data. We insist, however, that the objective is not to provide a complete unified theoretical reconstruction of the behavior of this photonic structure, but rather drive the reader's attention to the specificities found in the experimental observations and on the possible origin of these unique behaviors.

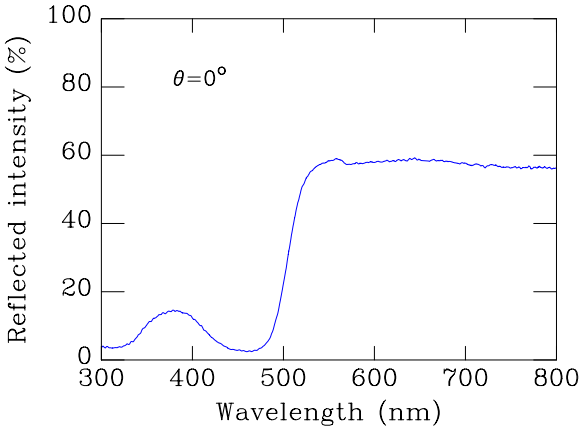

FIG. 5. (Color online) Light scattering by a yellow scale of the dorsal part of the wing of a *Troides magellanus*, at normal incidence and normal emergence. The reflected intensity is measured in units of the normal backscattered diffusion of a white standard reference.

The optical response of the yellow scales have been made quantitatively known by accurately measuring the light scattering from the yellow parts of the hindwings.

A. Methods

An Avaspec 2048/2 fiber optic spectrometer, with a combined halogen-deuterium source, was used for the measurements. Several configurations were exploited. The first one generates a specular reflection on the wings and contains the diffusion and the zero-order diffraction by the grating structure. The second one produces a total diffuse scattering of the incident light, which is accessed by collecting the scattered light in an integration sphere. In this geometry, the incidence beam is injected close to a normal incidence and the scattered light is collected over all the emergence and azimuthal directions and analyzed in the spectrometer. The third one defines a bidirectional measurement where, for a fixed angle of incidence, diffracted wavelengths are searched at specific nonspecular emergences. Finally, a special "backscattering" geometry was also mounted, where the probe fiber is, by construction, parallel to (and surrounded by) illumination fibers. In all these configurations, the reflected intensity is compared to the intensity scattered from a standard diffusive white polytetrafluoroethylene reference (Avaspec).

We must note that the normal incidence on the wing is not exactly the normal on the wing scales, as these can be implanted at some angle with the wing membrane, and this must be accounted for in the measurement interpretations. With this butterfly, the scales are relatively flat and nearly parallel to the wing membrane (the mismatch being estimated to be about α=8°, the normal to the scale being slightly displaced towards the head of the insect).

B. Normal backscattering

Figure 5 shows the result of the simple normal illumination and normal pickup experiment, a measurement which combines specular and backscattering configurations. Three distinct features of the resulting spectrum should be men-

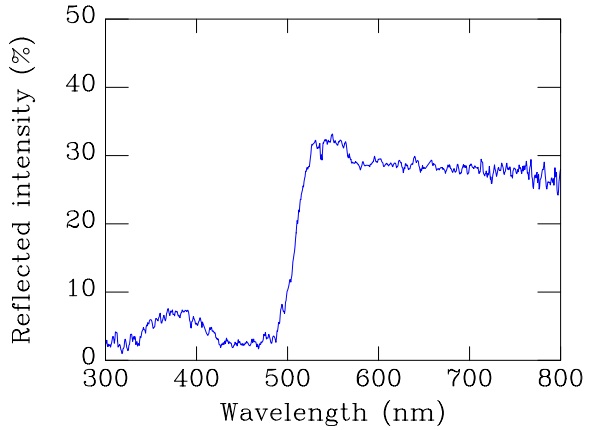

FIG. 6. (Color online) Light scattering by a yellow scale of the dorsal part of the wing of a *Troides magellanus*. The reflected light is collected over all emergence directions in an integration sphere. The reflected intensity is measured in units of the hemispheric diffusion of a white standard reference.

tioned. (1) First, the reflectance is constant over all visible wavelengths from 520 to 800 nm, while we note an abrupt fall for shorter wavelengths. The "blue" hole in the spectrum leads to the strongly saturated yellow coloration observed near normal incidence. This selectivity should be associated with the papiliochrome absorption. A careful examination of individual scales under the optical microscope in reflection and transmission modes (both under normal incidence) indicates that the yellow pigmentation is particularly strong in the ridges of the scales, an observation which suggests that the papiliochrome is directly incorporated in the bulk of the triangular ridge described above. (2) The second feature is the weak band near 380 nm, at the edge of the (human) visible spectrum. This band adds some violet component to the reflected light, but the desaturation effect is difficult if not impossible to perceive with the naked eye. This feature is related to the selectivity of the papiliochrome pigment, but a structural, nonabsorptive, effect should also be tentatively considered (see below). (3) Finally, one should also mention the small enhancement of reflectance at the edge of the yellow plateau, between 520 and 560 nm. This range of the visible spectrum is traditionally qualified as "yellowish green" and will be shown below to be associated with the papiliochrome fluorescence.

C. Diffuse scattering

The diffuse scattering spectrum, obtained from a male *Troides magellanus* hindwing (dorsal side) in a yellow region is shown in Fig. 6. This spectrum is not very different from the normal-incidence reflectance spectral distribution. The "supplementary" reflectance at the edge of the constant plateau is somewhat more easily visible, and can be more accurately identified as producing a dominant wavelength near 540 nm. The similarity between a normal backscattered spectrum and a total hemispherical reflection is expected for a wide-angle pigmentary diffusion or when no reflected beam other than specular occurs by diffraction. The latter condition essentially requires that the inhomogeneity of the scatterer occurs on a scale smaller than the incident radiation wavelength.

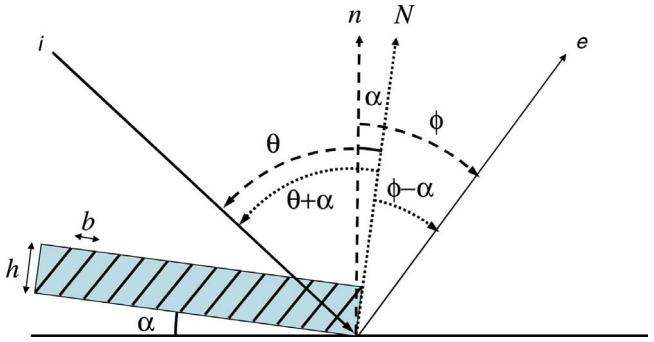

FIG. 7. (Color online) Scale and wing angular coordinates are different because each scale is implanted at an angle α on the wing basal plane. θ and ϕ are the experimental incidence and emergence angles, measured from the wing plane normal n. N is the normal to the plane of a scale. b is the grating parameter, measured parallel to the scale, and h is the height of a ridge.

D. Diffraction

The optical devices "engineered" on each scale of the hindwings produces diffraction of the incident light because the array of microribs forms a one-dimensional grating with period $b=261$ nm in the direction of the edge of the ridges. For a beam of wavelength λ, impinging on the scale under an incidence θ, in a plane parallel to the ridges, the angles of emergence ϕ of the diffracted beams is given by the expression [18] (see Fig. 7)

$$\sin(\phi-\alpha)=\sin(\theta+\alpha)+m\frac{\lambda}{b} \tag{1}$$

where m is a positive or negative integer. This formula is written under the assumption that the grating makes an angle α with the horizontal in the measuring (wing) coordinates (see Fig. 7). The implantation angle α is, on the average, found close to 8° for the *Troides magellanus* yellow scales.

The integer m should be chosen so that the resulting value of $\sin(\phi-\alpha)$ is smaller than unity. The special value $m=0$ describes the specular reflection, which does not produce any color separation in the emerging light, since (in the scale coordinates) the emergence angle is equal to the incidence angle whatever the incident wavelength λ. Different values of m produce diffraction for which the emergence angle varies with the wavelength.

In the diffraction produced by a grating, only a few orders are present in the far field, the others giving rise to evanescent waves: with a grating invariant under a translation of length $b=261$ nm, a wavelength larger than 2×261 nm $=522$ nm (in the green-yellow plateau) can never produce any diffracted beam other than specular [for $\lambda/b>2$, whatever values of θ and $m\neq0$, the quantity $|\sin(\phi-\alpha)|$ will always be larger than 1]. With such a grating, no diffraction can take place for wavelengths larger than about 520 nm (green). Under normal incidence ($\theta=0$), no diffracted beam can occur for $m\neq0$ if the wavelength λ is larger than the

grating step $b=261$ nm (otherwise, again, $|\sin(\phi-\alpha)|$ would exceed the sine limit). So, for normal illumination, diffraction can never occur in any of the visible or even in the near-ultraviolet ranges. This is part of the reason why the integrating-sphere reflectance measurement produces a spectrum very similar to the normal backscattering with such a fine grating: the integrating-sphere measurements only contains normal backscattering and the (angularly unstructured) diffused reflection. The other part of the reason is that, in the transverse direction, across the ridges, we have another grating, but its step (with $b_\perp=1400$ nm) is rather long, so that it produces essentially isolated-scatterer diffraction, which is widely spread over all emergence angles.

With the fine grating found in this butterfly, things are becoming more interesting if the angle of incidence is made larger, because the $m=-1$ starts providing beams in the visible range. For instance the "blue" color which complements the yellow hue of the scales (say at 450 nm) makes its appearance if the angle of incidence is larger than $\theta=38.4°$, in which case the $m=-1$ diffraction directs it at a very grazing emergence angle, near $\phi=-82°$ [see Eq. (1): the diffracted light emerges parallel to the scales]. The exact backscattering of this wavelength occurs when the angle of incidence is $\theta=51.5°$. This is roughly the situation met in the lower part of Fig. 1, where a strong bluish-white backscattering is observed at large incidences.

The experimentation of the properties of the grating can be carried out by means of an exact backscattering measurement. Here we set the measuring geometry in such a way that $\phi=-\theta$, which means that the diffracted light takes back the same path as the incident beam, in the reversed direction. Then, from Eq. (1), we should see a strong enhancement of the intensity return at wavelengths such that

$$\lambda = \frac{2b}{(-m)} \sin(\theta+\alpha). \tag{2}$$

From this formula, it can be expected that with increasing angle θ, the $m=-1$ backscattered wavelength λ should be redshifted but would not pass over the limiting value $\lambda=2b$. This is exactly what Fig. 8 shows, at least for large incident angles. Indeed, for $\theta=45°$, Eq. (2) predicts a backscattered wavelength $\lambda(45°)=416$ nm, and, similarly, $\lambda(60°)=484$ nm and $\lambda(70°)=510$ nm, all in good agreement with the high-reflection bands shown in the corresponding panels in Fig. 8.

This analysis is, however, apparently less convincing when addressing smaller incidence angles: $\lambda(30°)=321$ nm and, even more obviously, $\lambda(0°)=72$ nm cannot provide an interpretation of the weak broad reflection band that remains near 380 nm. This spectral feature, which appear in the visible range at normal incidence, cannot arise from diffraction on the microribs grating.

As the absence of diffraction near normal incidence can be expected, its absence at the edge of the (human) visible spectrum near 380 nm for $\theta=30°$ is more intriguing. In the same respect, the specular order ($m=0$) is not observed to receive any intensity. Furthermore, as Fig. 9 shows, there is a strong difference between the measurements of the backscattering for incidences towards the body of the insect and from the body to the end of the wing. This asymmetry is not

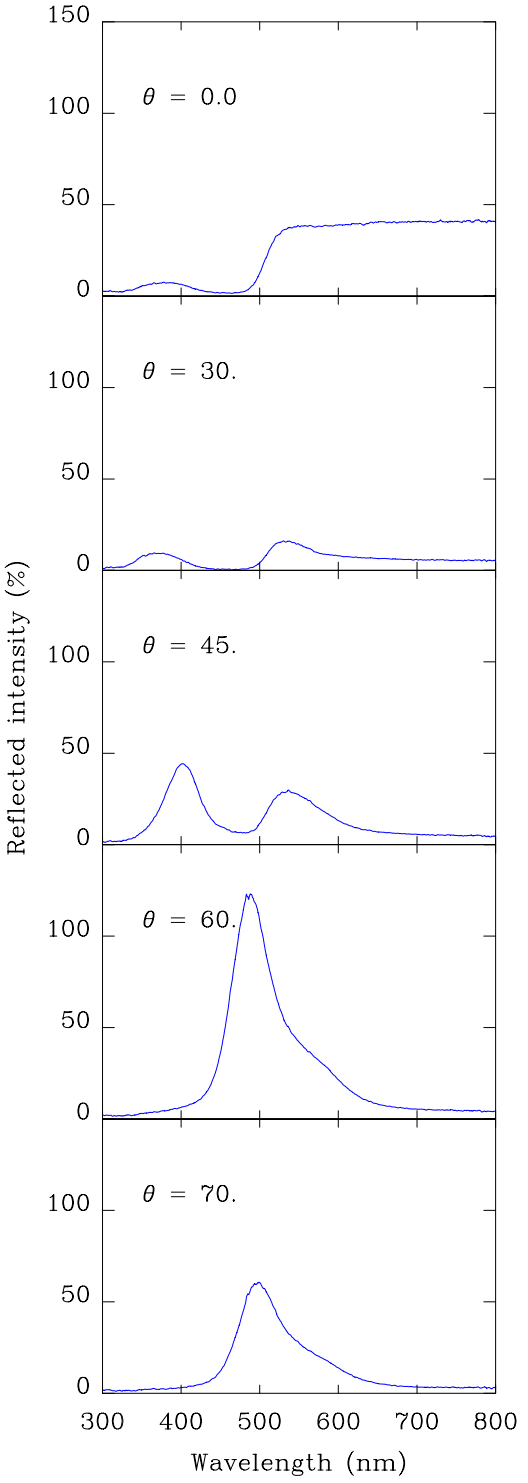

FIG. 8. (Color online) Backscattering spectra of the yellow scales of the male *Troides magellanus* for different incidence angles θ (in degrees).

contained in expressions such as Eq. (1) or Eq. (2), which only reflect the discrete translational invariance of the ridges and do *not* depend on such details as the shape of the scatterers in each of the grating's unit cell. The diffracted intensities, however, do depend on these details. The blue-green diffracted intensity is apparently maximum at grazing incidences and emergences, such as for the backscattering near

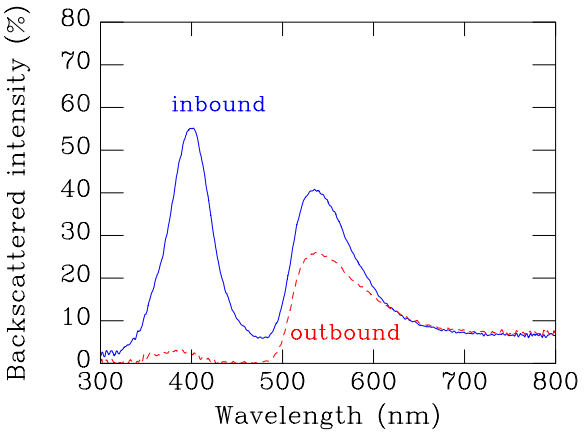

FIG. 9. (Color online) Backscattering diffraction by a yellow area of the hindwing of a male *Troides magellanus*. The source and pick-up fibers are set in a plane parallel to the ridges and containing the normal to the wing. The solid line ("inbound") shows the backscattered spectrum for an incident beam directed from the rear of the butterfly towards the insect's body. The dashed line ("outbound") is for an incident beam directed in the opposite direction.

$\theta=60°$ and vanishes rather rapidly for other geometries, including reverse illumination.

The microribs array can be modeled as a set of tiny mirrors which make an average angle of $\beta=61°$ with the line at the top of the ridges, their normal being oriented towards the up rear of the butterfly (see Fig. 7). Such a structure can be viewed as a blazed grating, similar to that recently discovered by Ingram on *Lamprolenis nitida*, a New-Guinea butterfly [19]. The blaze angle provides a high-intensity envelope for the diffracted beams which match the reflectance law about the normal to the microribs "mirrors." Because the scales are implanted at an angle α to the wing plane, the normal to the microribs make an angle $\beta-\alpha$ with the normal to the wing, so that, for a beam incident under an angle θ (in the wing coordinates), the incidence angle on the tiny microribs mirrors is $\beta-\alpha-\theta$ and the specular direction is $\phi=\theta-2(\beta-\alpha)$. Whenever the diffracted beam matches this direction, it will be reinforced. The tolerance for deviating from this condition is related to size of the microribs, which can be considered as a "window" from which the emerging wave is emitted. The length of a microrib is (from Fig. 10) $\Delta=h/\sin\beta\simeq 4300$ nm and the emergence angle uncertainty is

$$\sin\delta\simeq\frac{\lambda}{\Delta}. \tag{3}$$

δ is the angular spread of the enhanced intensities about the specular microrib reflection. For blue light at $\lambda=400$ nm, $\delta\simeq 5°$. We can visualize the blazing effect by calculating, as a function of the incident wavelength and incident angle, the "specularity index" defined as

$$\rho(\lambda,\theta)=\exp\left[-\frac{|\phi(\lambda,\theta)-\theta+2(\beta-\alpha)|^2}{2\delta^2}\right] \tag{4}$$

which expresses the conditions, according to the wavelength λ and the incidence angle θ, where the diffraction by the

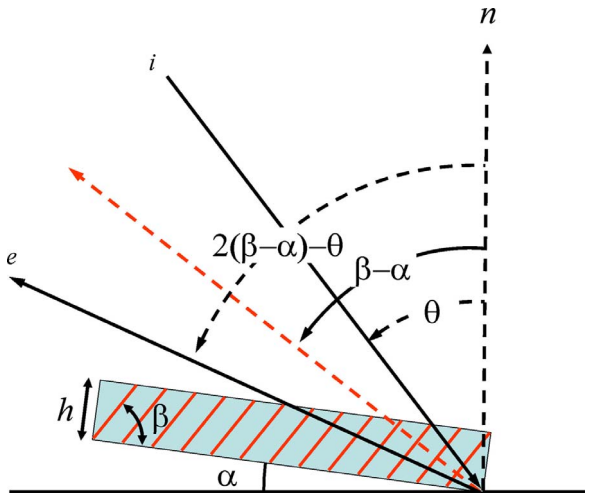

FIG. 10. (Color online) Periodically repeated microribs define a blazed grating, able to put a maximal amount of energy in a well-defined diffraction order. With *Troides magellanus*, this means switching off the specular $m=0$ order and direct the scattering into the $m=-1$ backscattered beam, if a local specularity condition is met on each microrib. The dashed line at an angle $\beta-\alpha$ from the wing normal is the normal to the microribs. β is the slant angle of the microribs with respect to the scale plane and α is the angle between the scale and the wing.

microribs grating is most intense. The specularity index varies between 0 and 1 and is large only when the emergent beam matches closely the blazing condition (specular reflection on the microribs plane). The use of a Gaussian shape is arbitrary: other spreading functions would give similar results. In this expression, $\phi(\lambda,\theta)$ is the emergence angle calculated by using Eq. (1).

Figure 11(a) gives a representation of this specularity index $\rho(\lambda,\theta)$ for all incident angles θ and relevant wavelengths λ. Only the $m=-1$ value is shown: all other diffraction order (including $m=0$) are negligible (this means that this blazed grating can only produce $m=-1$ backscattered diffraction). The dark areas in Fig. 11(a) correspond to prevented diffraction, while the white areas indicate the wavelengths and incidence angles where a strong diffraction is allowed to occur, due to blazing condition matching. No diffracted intensity can be observed for wavelengths above 500 nm and only blue and green diffraction can be observed, turning—when occurring—the yellow pigmentary scattering of papiliochrome into a white signal. On the other hand, only angles well above 30° can be used for illumination in order to produce a strong emerging grazing diffracted beam.

This matches very well the conditions under which, according to observations, the diffracted beam is apparent: Fig. 11(b) essentially repeats the experimental information provided in Fig. 8, but with an augmented amount of data, in order to provide a more complete two-dimensional map of the observed reflection. The reflected intensity, described as a function of the incident wavelength and angle, show essentially two enhancement regions: the first one, labeled "diffraction" arises from the direct scattering on the microribs grating, and matches the theoretical blazing enhancement shown on Fig. 1(a) of the same figure, and another one,

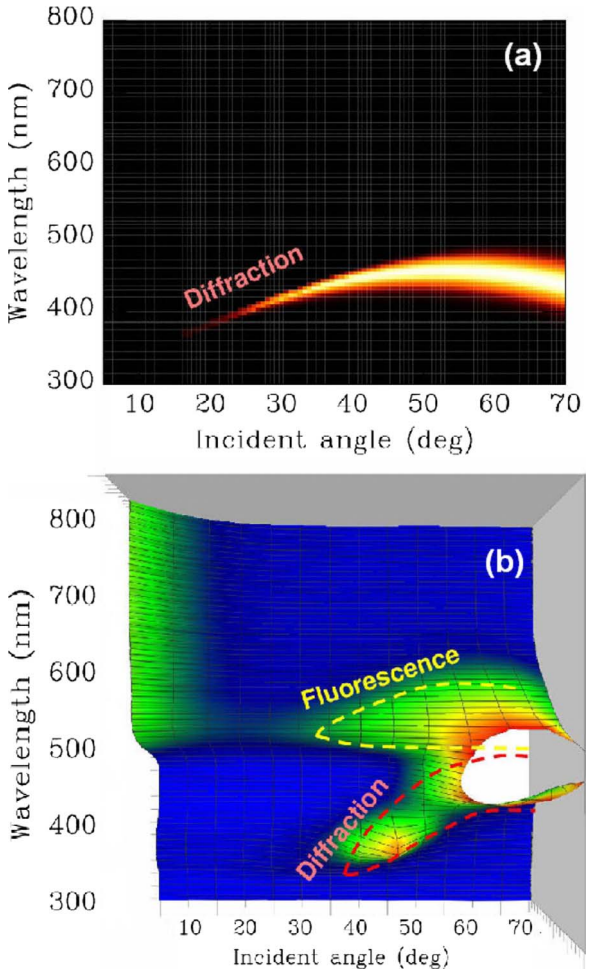

FIG. 11. (Color online) (a) Theoretically determined wavelengths and incidences for which the slanted microribs grating produces intense $m=-1$ diffraction, under backscattering conditions. In the dark area, no emerging light occurs, either because the direction does not match a possible diffraction, or because of intensity suppression under the slanted orientation of the microribs. Diffracted emergence only occur in the strong white areas at large incidence angles in the blue-green spectral range. (b) Experimental observation of the light backscattering on the butterfly wings. The diffracted intensities (region labeled "diffraction") occur at wavelengths and under illumination conditions which match very reasonably the blazed grating predictions described in (a). The region labeled "fluorescence" match the papiliochrome fluorescence wavelength. It does not show in the calculated map (a) because fluorescence is not considered there. Fluorescence increases in intensity with increasing incidence angles, so that both diffraction and fluorescence appear strong under the same illumination angles.

indicated by the label "fluorescence" cannot be explained by grating diffraction, but, as we will see below, matches a resonant emission of fluorescence from the papiliochrome pigment.

E. Fluorescence

In males and females *Troides magellanus*, the diffuse yellow coloration of the hindwings is produced by a pigment,

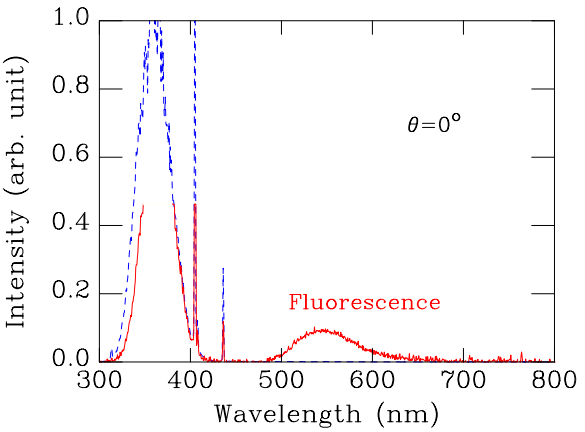

FIG. 12. (Color online) Fluorescence spectrum of the yellow scale of a *Troides magellanus*. The illuminating source is a Wood lamp with a spectrum confined at wavelengths shorter than 450 nm (shown as a dashed line, for comparison). The solid line is the light reflected by a yellow area on the hindwing. Note the fluorescence in the yellow-green region.

termed "papiliochrome" [20]. This pigment is also found in other Papillionidae, in many parts of the world. The active chemical compound releasing a vivid yellow color is fluorescent: under the light of a Wood lamp (which contributes most of its radiation near 350 nm), the yellow-green emission by the hindwings is easily seen in the dark. As Fig. 12 shows, the color of the fluorescence appears near 540 nm and overlaps the yellow coloration of pigmentary origin. In fact, the visual effect produced by the fluorescence is very close to the effect obtained in artificial fluorescent inks, where the coincidence of the pigmentary color and the conversion of the blue and ultraviolet light leads to a strong reinforcement of the color brightness.

The spectrum in Fig. 12 was obtained by the same spectrophotometer that produced the reflection measurements. The Wood lamp (spectrum drawn as dotted lines) was used as a source, and the spectrometer accumulated the visible and ultraviolet response from the wing in "scope" mode, that is, without normalizing the accumulated energy to any reference standard. The response spectrum (solid line in Fig. 12, saturated near 0.45) contains both the spectral emission of the source and the new band, near 540 nm, which corresponds to the papiliochrome fluorescence. Note, on the dashed-line spectrum, that the Wood lamp contains no frequency component in the green-yellow region.

The measurement of the fluorescent band allows one to identify the second component of the backscattering spectra in Fig. 8 and Fig. 11(b): whatever the angle of incidence, the dominant wavelength in this region is very close to 540 nm, so that a large part of this band can be explained by a fluorescent conversion in the pigment. An intriguing fact, which shows up on the different spectra shown in Fig. 8 and in the overlap of the "diffracted" and "fluorescence" regions in Fig. 11(b) is that the fluorescence *increases in parallel* with the increase of the blue-green diffracted light. The correlation between the enhancement of fluorescence and diffraction is another remarkable feature of the butterfly scales that calls for some explanation.

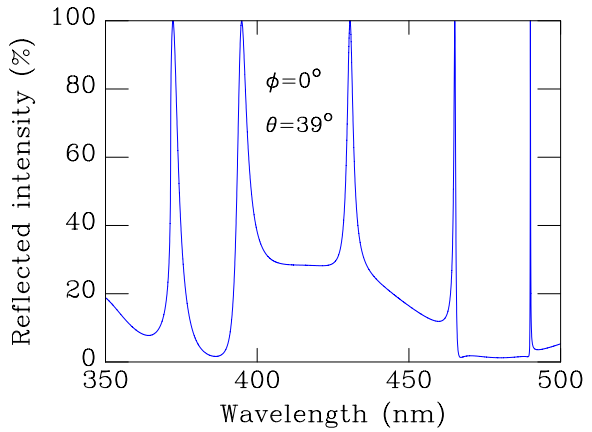

FIG. 13. (Color online) Reflectance of a model chitin guiding slab with dimensions comparable to the *Troides* scale ridges, wearing a grating similar to the array of microribs.

Optical microscopy indicates that, in a yellow scale, the pigment is located in the triangular-shaped rod which constitutes the core of the ridges. The efficiency of the fluorescence requires that the blue-ultraviolet light absorbed by the pigment penetrates this rod and stays there for enough time to be absorbed and converted. This incident light must then cross the grating of the microribs. The system of rods with microribs resembles an optics fiber, with a triangular section, wearing a Bragg coupler, which is often designed, in photonics technology, as a grating drawn on the surface of the fiber with a pitch in the fiber axis direction. In order to see that the microribs grating can actually act as a Bragg coupler for short wavelengths, the reflectance of a chitin slab whose thickness corresponds to an average value of the thickness of the rods (d=550 nm) was calculated. We added on one of its surface a grating with a period a=228 nm, which is the period of the microribs along their own normal (not along the ridge top line). The microribs themselves are represented by rectangular chitin rods 88 nm wide and 144 nm high (values deduced from electron microscopy). A detailed spectrum in a narrow "blue" range is shown in Fig. 13. The *very narrow, asymmetric* lines of large amplitude in the reflectance spectrum are "Fano resonances" [21], which indicate a possible exchange of energy between the incident waves and the guided modes confined in the scale ribs. This phenomenon is similar to the coupling of ultraviolet light in the white filamentary hair of the edelweiss, as evidenced earlier [22] and its application to optics fibers injection is described as the "optic fibers Bragg coupler" [23]. The light propagating several micrometers along the triangular ridges, which contain the papiliochrome pigment, can interact with the pigment much more effectively, as compared with the case when the light just crosses the ridges roughly 1 micron thick.

IV. CONCLUSION

The male birdwing butterfly *Troides magellanus* presents two peculiarities that call for a quantitative physical analysis: (1) the blue-green diffraction which complements the yellow pigmentary diffusion to produce a white iridescence at grazing emergences and (2) the emission of a yellow-green fluorescence that appears with the illumination by a blue, violet, or ultraviolet light. These visual effects appear to be correlated, as they both occur in the same illumination conditions that produce the iridescent signal. The analysis reported in this paper underlines the importance of a natural grating in both processes.

The yellow scales of this butterfly bear clearly visible ridges, with triangular section, that contain a fluorescent papiliochrome pigment. The upper sides of these ridges are striped by protruding microribs that form a one-dimensional grating which is shown to play a central role in the scales optical properties. The orientation of the groves and ridges of this grating is of prime importance to explain the optical properties of the yellow scales. The periodicity of the repetition of the microribs along the ridges explain the appearance of the backscattered $m=-1$ diffraction beam, and the slant of the microribs with respect to the scale plane explains the intensity enhancement at grazing emergences. The slant of the microribs actually turns the ridges into a "blazed" grating, optimized to send most of the diffracted energy into this $m=-1$ order, effectively suppressing the specular $m=0$ diffraction. The high aspect ratio of the microribs also explains the well-defined angular definition of the outgoing light.

The fluorescence of this butterfly is another important feature. The absorption of blue to ultraviolet light leads to a reinforcement of the yellow brightness of the hindwings by adding energy to the greenish-yellow diffuse scattering caused by the papiliochrome pigment. It is observed that the fluorescence is enhanced for illuminations that produce the blue-green grazing iridescence and our analysis suggests that the microribs grating also influences the fluorescence efficiency. The energy transfer is similar to that occurring in Bragg couplers designed to inject propagating light in the guided modes of optic fibers in optical communication devices. The signature of this energy transfer is the presence, in the ultraviolet-blue region of very narrow Fano resonances, appearing in the calculated reflectivity of a model guiding device similar in structure and size to the scale ridges. The examination of the profile width of these resonances indicates that the energy transfer is enhanced in the illumination conditions which lead to the blue-green grazing-emergence diffraction and this explains the observed correlation between the diffraction and the fluorescence.

The use of blazed gratings in nature is not likely to be exceptional: another quite remarkable example was already described by a butterfly from the mainland Papua New Guinea, which actually shows two imbricated blazed gratings, on the same scale, acting on different spectral regions [19]. Other similar structures have also been identified on the abalone shell [24] and on the setae of an isopod (Crustacea). Natural Fano resonances seems to be less frequent [22].

The correlation between diffraction and fluorescence is most probably not a coincidence and has most probably a biological significance. The iridescence of the male *Troides magellanus* yellow wings, perceived only under a grazing emergence angle, is likely important for intraspecific recognition. As with many butterflies, the female, while larger than the male, displays a less conspicuous pattern of colors (though equipped with yellow fluorescent scales, a female

Troides magellanus does not show any iridescence). This indicates that the color brightness of the male—and its iridescence—can be useful for accelerating the male and female fruitful encounters, influencing positively the population growth. Since the iridescence is hidden if the illumination and the view point do not match the backscattering geometry described at length in the present paper, the mating signal is most of the time "confidential" and unknown to the butterfly's predators.

The way these signals are used in nature is still difficult to assess: it would be essential for biologists to investigate the wing beating mode, the butterfly changes of attitude during the flight, the wing movements while perching or basking (all time-dependent light manipulations) in order to better understand the contents of the emitted messages. It is important that none of the species in these fascinating tribe of butterflies proceeds towards extinction, not only because they represent in themselves a valuable genetic entity, but also because they most likely still hide further inspiriting physical mechanisms, which can be exploited only by studying these insects alive in their natural habitats.

ACKNOWLEDGMENTS

The work was supported in part by Grant No. EU6 BIOPHOT/NEST. The authors acknowledge the use of Namur Interuniversity Scientific Computing Facility (Namur-ISCF), a common project between the Belgian National Fund for Scientific Research (FNRS), and the Facultés Universitaires Notre-Dame de la Paix (FUNDP). V.L. was supported by the Belgian National Fund for Scientific Research (FNRS). M.R. acknowledges the support of the Belgian Fund for research in Industry and Agriculture (FRIA).

[1] B. D'Abrera, *Birdwing Butterflies of the World* (Lansdowne Press, Melbourne, 1975).
[2] M. Parsons, *The Butterflies of Papua New Guinea. Their Systematics and Biology* (Academic Press, San Diego, CA, USA, 1999).
[3] R. I. Vane-Wright, in *Butterflies Ecology and Evolution Taking Flight*, edited by C. L. Boggs, W. B. Watt, P. R. Ehrlich (The University of Chicago Press, Chicago, 2003), p. 477.
[4] B. d'Abrera, *Birdwing Butterflies of the World. New and Revised Edition* (Hill House Publishers, Melbourne, 2003).
[5] P. R. Ackery, R. de Jong, and R. I. Vane-Wright, in *Lepidoptera, Moths and Butterflies*, edited by N. P. Kristensen (Walter de Gruyter, Berlin, 1999), Vol. 1, p. 264.
[6] N. M. Collins and M. G. Morris, *Threatened Swallowtail Butterflies of the World. The IUCN Red Data Book* (IUCN, Gland, Switzerland, 1985).
[7] H. Matsuka, *Natural History of Birdwing Butterflies* (Matsuka Shuppan, Tokyo, 2001).
[8] G. Horvárth and A. Mocsáry, Természetrajzi Füzetek **23**, 160 (1900).
[9] C. Lawrence, P. Vukusic, and R. Sambles, Appl. Opt. **41**, 437 (2002).
[10] P. Vukusic and I. Hooper, Science **310**, 1151 (2005).
[11] H. Ghiradella, D. Aneshansley, T. Eisner, R. E. Silberglied, and H. E. Hinton, Science **178**, 1214 (1972).
[12] H. Tada, S. E. Mann, I. N. Miaoulis, and P. Y. Wong, Appl. Opt. **37**, 1579 (1998).
[13] P. Vukusic, J. Sambles, and H. Ghiradella, Photonics Sci. News **6**, 61 (2000).
[14] P. Vukusic, J. R. Sambles, C. R. Lawrence, and R. J. Wootton, Nature (London) **410**, 36 (2002).
[15] A. Argyros, S. Manos, M. C. J. Large, D. R. McKenzie, G. C. Cox, and D. M. Dwarte, Micron **33**, 483 (2002).
[16] S. Yoshioka and S. Kinoshita, Proc. R. Soc. London, Ser. B **271**, 581 (2004).
[17] Z. Vertezy, Z. Balint, K. Kertesz, D. Mehn, I. Kiricsi, V. Lousse, J.-P. Vigneron, and L. Biro, Microscopy and Analysis **18**, 25 (2004).
[18] J. P. Vigneron and V. Lousse, Proc. SPIE **6128**, 61281G (2006).
[19] A. L. Ingram, V. Lousse, A. R. Parker, and J. P. Vigneron, J. R. Soc. Interface, doi:10.1098/rsif.2008.0227 (2008).
[20] E. A. C. Cockayne, Trans. Entomol. Soc. London A, **71**, 1 (1924).
[21] U. Fano, Phys. Rev. **124**, 1866 (1961).
[22] J. P. Vigneron, M. Rassart, Z. Vértesy, K. Kertész, M. Sarrazin, L. P. Biró, D. Ertz, and V. Lousse, Phys. Rev. E **71**, 011906 (2005).
[23] A. Othonos and K. Kalli, *Fiber Bragg Gratings: Fundamentals and Applications in Telecommunications and Sensing* (Artech House, London 1999).
[24] J. Wang, X. J. Peng, and C. Yuan, in *Advanced Biomaterials VI*, edited by E. A. Armanios, Y. W. Mai, G. M. Newaz, F. H. Wohlbier, Key Engineering Materials Vol. 288 (Trans Tech Publications, Switzerland, 2005), p. 669.